



HAL
open science

Ab Initio Molecular Dynamics Study of Alignment-Resolved O₂ Scattering from Highly Oriented Pyrolytic Graphite

Alejandro Rivero Santamaría, Maite Alducin, Ricardo Díez Muiño, J. Iñaki
Juaristi

► **To cite this version:**

Alejandro Rivero Santamaría, Maite Alducin, Ricardo Díez Muiño, J. Iñaki Juaristi. Ab Initio Molecular Dynamics Study of Alignment-Resolved O₂ Scattering from Highly Oriented Pyrolytic Graphite. *Journal of Physical Chemistry C*, 2019, 123 (51), pp.31094-31102. 10.1021/acs.jpcc.9b09774. hal-04087337

HAL Id: hal-04087337

<https://hal.science/hal-04087337>

Submitted on 8 Mar 2024

HAL is a multi-disciplinary open access archive for the deposit and dissemination of scientific research documents, whether they are published or not. The documents may come from teaching and research institutions in France or abroad, or from public or private research centers.

L'archive ouverte pluridisciplinaire **HAL**, est destinée au dépôt et à la diffusion de documents scientifiques de niveau recherche, publiés ou non, émanant des établissements d'enseignement et de recherche français ou étrangers, des laboratoires publics ou privés.

Ab Initio Molecular Dynamics Study of Alignment Resolved O₂ Scattering From Highly Oriented Pyrolytic Graphite

Alejandro Rivero Santamaría,^{*,†,‡} Maite Alducin,^{*,†,‡} Ricardo Díez Muiño,^{*,†,‡}
and J. Iñaki Juaristi^{*,¶,†,‡}

[†]*Centro de Física de Materiales CFM/MPC (CSIC-UPV/EHU), Paseo Manuel de Lardizabal 5,
20018 Donostia-San Sebastián, Spain*

[‡]*Donostia International Physics Center DIPC, Paseo Manuel de Lardizabal 4, 20018
Donostia-San Sebastián, Spain*

[¶]*Departamento de Física de Materiales, Facultad de Químicas, Universidad del País Vasco
(UPV/EHU), Apartado 1072, 20080 Donostia-San Sebastián, Spain*

E-mail: arivero@dipc.org; maite.alducin@ehu.eus; rdm@ehu.eus;
josebainaki.juaristi@ehu.eus

Abstract

We present ab initio molecular dynamics simulations based on density functional theory to study the alignment dependent scattering of O₂ from highly oriented pyrolytic graphite (HOPG). Results are obtained for 200 meV O₂ molecules with different alignments impinging with an angle of incidence measured from surface normal of 22.5° on a thermalized (110 and 300 K) graphite surface. The choice of these initial conditions in our simulations is made in order to perform comparisons with recent experimental results on this system. Our results show that a lower number of molecules initially aligned normal to the surface is reflected in the scattering plane than of molecules initially aligned parallel to the surface. This is not due to an increase of the trapping of end-on aligned molecules, but due to the fact that a large amount of them are scattered out of plane. Additionally, we find that the final translational energy of end-on molecules is around 10% lower than that of side-on molecules. We show that this is due to a more efficient energy transfer from the translational degree of freedom to internal degrees of freedom for end-on molecules, and not due to a more efficient energy transfer to the surface. The results of our simulations are in overall agreement with the experimental observations regarding the alignment dependence of the in-plane scattering probabilities and the energy loss of the reflected molecules.

1 Introduction

The study of gas/surface dynamics is relevant to understand chemical reactions at surfaces with applications in heterogeneous catalysis.¹⁻³ In this respect, it is crucial to gain knowledge on the characteristics of the molecule-surface interaction, for which molecular beam experiments constitute an invaluable tool.⁴ In particular, by controlling the geometry of the incident molecule, information can be obtained of the so-called steric effects and the anisotropy of the interaction potential.⁵ For heteronuclear diatomic molecules this has led to the investigation of the orientation effect, i. e., differences between the head and tail orientations of the molecules respect to the surface. Typically, these heteronuclear molecules present an attractive and a repulsive end with the

subsequent anisotropy of the interaction potential, which induces an orientation dependent reactivity and affects the measured angular distributions of the scattered molecules. Since the pioneering experiments by Kleyn and coworkers for the NO/Ag(111) system,⁶ various experimental and theoretical works have been devoted to the study of the orientation effect in the scattering and reactivity of molecules such as NO and CO at different surfaces.⁷⁻¹¹ In the case of homonuclear molecules the alignment effect is measured which distinguishes the side-on and end-on collisions. Though not so intensively studied as the orientation effect, in the last years the interaction of aligned molecules with surfaces is increasingly receiving much attention thanks to recent advances in the experimental setups that allow to know how the stereochemistry and spin state of molecules influence the interaction dynamics and reactivity on different surfaces.¹²⁻¹⁶

Regarding the specific system studied here, there are several experimental¹⁷⁻²¹ and theoretical²²⁻³⁰ studies focused on the interaction of O₂ with highly oriented pyrolytic graphite (HOPG). The reason is the importance of this model system for understanding the behavior of carbon-based materials in different applications, such as, processes of burning phenomena in nature, coal gasification, reactions at nuclear reactor walls, and the degradation mechanism of the spacecraft vehicles shielding, among others. However, new information about the effect of the alignment of the incident O₂ could contribute to elucidate the involved mechanisms on the molecule-surface interaction that take place in the non-reactive scattering process. In this respect, recently, first experimental results on alignment-resolved O₂ scattering from HOPG have been published by Kurahashi et al,¹⁶ reporting the molecule alignment dependence of scattering distributions, energy loss and trapping probabilities at surface temperatures of 110 and 300 K and incident O₂ beam with translational energies between 0.08-0.25 eV. The experimental setup used by Kurahashi et al¹⁶ allows to detect the intensity of O₂ molecules scattered or desorbed from the HOPG surface with a fixed angle of 45° relative to the incidence beam. The authors report a marked alignment dependence of the scattering features associated mainly with the surface roughness seen by the incident molecule.

In order to contribute to the theoretical understanding of these experiments we have performed ab initio molecular dynamics (AIMD) calculations. The use of AIMD has the advantage that

is not necessary to obtain a previous potential energy surface (PES) because the energies and forces during the dynamics are determined on the fly at the density functional theory (DFT) level. Also, allowing surface atom movement, a better description of the molecule-surface interaction, including molecule-surface energy exchange and temperature effects can be effectively achieved.

The paper is organized as follows. Section 2 describes the theoretical method and the practical implementation of the AIMD dynamics simulations on the present system. The methodology is applied in Sec. 3 to study the alignment effect on the scattering of O₂ from the HOPG surface at 100 and 300 K. An extensive comparison of our results and the recent experimental observations by Kurahashi and Kondo is presented at the end of Sec. 3. Finally, a summary of the results and the main conclusions of this work are provided in Sec. 4.

2 Computational details

Spin polarized ab initio molecular dynamics (AIMD) calculations were performed with the DFT based Vienna Ab Initio Simulation Package (VASP)^{31,32} using the Perdew-Burke-Ernzerhof (PBE)³³ exchange-correlation functional, together with the DFT-D3(BJ) dispersion correction^{34,35} that amends the inadequacy of PBE to describe van der Waals (vdW) interactions. The ionic cores were described with the projector augmented wave (PAW) method³⁶ implemented in VASP.³⁷ A gaussian smearing of 0.05 eV was used for the electron occupancies and the plane wave expansion was cut at a kinetic energy of 430 eV.

The lattice parameters calculated for bulk graphite using a (16×16×8) Monkhorst-Pack sampling³⁸ of the Brillouin zone are $a = b = 2.47$ Å and $c = 6.70$ Å. Next, the graphite (0001) surface was described by a three layer (3×3) supercell (54 atoms of C) separated from its periodic image by 16 Å of vacuum along the surface normal. In all the calculations performed with this supercell, the Brillouin zone was sampled with a (5×5×1) Monkhorst-Pack mesh. After surface relaxation the interlayer distance remains as 3.35 Å. These values are in agreement with experimental³⁹ and previous theoretical DFT-D3(BJ)^{40,41} results (3.34 and 3.41 Å, respectively). Also the binding en-

ergy of 5.92 eV and bond length of 1.23 Å calculated for the O₂ molecule aligned parallel to the surface and located at a height of 7 Å agree reasonably well with the experimental values (binding energy of 5.116 eV and 1.21 Å, respectively).⁴²

Scattering of O₂ from the HOPG surface thermalized at 110 and 300 K is simulated with classical trajectories using constant-energy AIMD calculations. The O₂ incidence conditions, in which the zero point energy is neglected, correspond to a (translational) kinetic energy of 0.2 eV with the velocity vector of the O₂ center of mass defined by a fix polar angle $\theta_i=22.5^\circ$ and a random azimuthal angle φ_i that is sampled within the -90° to 90° interval. All trajectories start with the center of mass of the molecule at 7 Å from the surface in order to assure negligible molecule-surface interaction at the beginning of the trajectory. The initial O₂ internuclear distance was set to the theoretical equilibrium bond length $r_e=1.23$ Å. The molecular alignment angles (θ , φ) were referred to the scattering plane, which is defined in each trajectory by the surface normal and velocity vector as shown in Figure 1. Three different initial alignments of the O₂ molecule were used: P_X ($\theta=90^\circ$, $\varphi=90^\circ$), P_Y ($\theta=90^\circ$, $\varphi=0^\circ$), and P_Z ($\theta=0^\circ$, $\varphi=0^\circ$). In other words, P_X corresponds to the molecular axis aligned parallel to the surface and perpendicular to the scattering plane, P_Y to the molecular axis aligned parallel to the surface and inside the scattering plane, and finally, P_Z to the molecular axis aligned perpendicular to the surface.

Following a standard procedure in gas-surface dynamics simulations,⁴³⁻⁵⁰ the surface temperatures were described within our constant energy AIMD calculations by selecting the initial positions and velocities of the moving HOPG surface atoms (those in the two topmost layers) from a large set of configurations that constitute a canonical ensemble. This procedure is a reasonable approximation for the usual short simulation times of interest (4 ps in our simulations).⁴⁷ In our case, the initial HOPG configurations are selected for each surface temperature and trajectory, from a canonical AIMD calculation that was run for 10 ps with a time step of 1 fs using the Nosé-Hoover thermostat^{51,52} implemented in VASP. This procedure guarantees that the initial surface temperature in the simulations coincides with the experimental temperature, within the statistical uncertainty due to the limited number of trajectories.

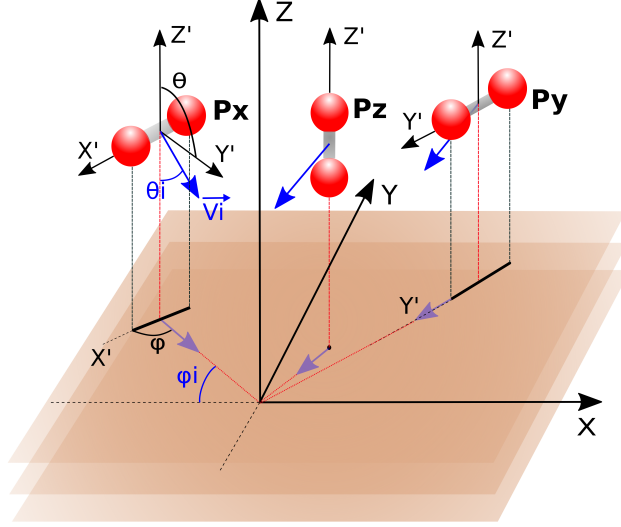


Figure 1: Coordinate system and sketch of the three initial alignments (P_X , P_Y , P_Z) used in the AIMD simulations of one O_2 molecule impinging over the HOPG surface. Blue arrows and symbols refer to the incidence velocity vector of the O_2 center of mass.

Finally, under these conditions 200 AIMD trajectories per initial O_2 alignment (P_X , P_Y , P_Z) and per surface temperature (110 and 300 K) were carried out using the Beeman algorithm⁵³ implemented in our modified version of VASP.^{47,54–56} The maximum propagation time was 4 ps with a time step of 1 fs. Two possible exit channels were observed, namely, scattered and adsorbed molecules. We estimated that the dissociative adsorption of O_2 is endothermic by ~ 1.89 eV. Thus this channel is not open under our simulation conditions. The molecule was considered reflected when the distance from the HOPG surface to the O_2 center of mass exceeded 8 \AA and trapped if after 4 ps the previous condition was not reached. The total energy was well conserved in the trajectories with a maximum average error of ~ 20 meV.

Reflected trajectories were discriminated according to the final angle of the center of mass velocity vector respect to the surface normal (outgoing polar angle (θ_s)) and its deviation respect the scattering plane (outgoing azimuthal angle (φ_s)). Molecules for which the deviation φ_s from the scattering plane is equal or smaller than 5° were considered in-plane. Angular distributions of the reflected O_2 were calculated using constant intervals of 5° and 10° for the azimuthal and polar angular distributions, respectively. The probability errors were calculated by the usual formula for binomial distributions. The final energy distribution of the reflected molecules was obtained after

a classical determination of translational, vibrational, and rotational energies.

3 Results and Discussion

3.1 Scattering probabilities and angular distributions

Table 1 summarizes the total and in-plane scattering probabilities obtained from our AIMD simulations for each incidence alignment and surface temperature. Total probabilities are calculated considering all the reflected trajectories (i.e., irrespective of the outgoing polar (θ_s) and azimuthal (φ_s) angles), while in-plane probabilities refer to molecules reflected with an azimuthal deviation from the scattering plane $\|\varphi_s\| \leq 5^\circ$. The results show that the total scattering probability is almost independent of the initial alignment of the molecule and surface temperature. In all cases, approximately 8 of 10 molecules are reflected, while the other 2 remain trapped on the surface after 4 ps of simulation time. The analysis of the reflected trajectories reveals that most of the scattered molecules suffer a single collision with the HOPG surface. The percentage of trajectories that are reflected after one rebound is also presented in Table 1. In addition to this direct scattering, there are few trajectories in which the molecule is clearly trapped on the surface, experiencing multiple collisions before being finally reflected.

Considering the small percentage of both the trapped and the multiple-scattered events, the scattering of O₂ from HOPG can still be viewed as a rather direct process. In this respect, our results are both compatible with the analysis of the experimental scattering distributions (based on a hard cube model) suggesting that the process is dominated by direct scattering^{18,19} and the small amount of trapping reported in recent experiments by Kurahashi and Kondo.¹⁶ From the theoretical side, trapping of O₂ on the HOPG surface was also obtained in molecular dynamics simulations performed on a Lennard-Jones PES²⁹ for incidence energies of around 90 to 650 meV and 300 K of surface temperature. The larger percentage of trapped molecules in that work ($\sim 27 - 70\%$) is attributable to the larger incidence angle of 45° used in those simulations. Our percentage of $\sim 20\%$ would be consistent with the trapping decrease observed by these authors when increasing

Table 1: Total and in-plane scattering probabilities (%) for the three molecular initial alignments and two surface temperatures considered in the AIMD simulations. The percentage of trajectories that are reflected after one single collision with the surface is within parenthesis.

$T(\text{K})$		P_X	P_Y	P_Z
110	total	82.5±2.7 (71.0)	84.5±2.6 (71.0)	81.5±2.7 (62.0)
	in-plane	42.5±3.5 (38.0)	36.0±3.4 (35.0)	27.0±3.1 (23.5)
300	total	80.5±2.8 (60.5)	84.5±2.6 (60.0)	79.0±2.9 (51.0)
	in-plane	43.0±3.5 (35.5)	44.0±3.5 (35.0)	26.5±3.1 (19.0)

the incidence energy. More recently, molecular dynamics simulations performed on an improved Lennard-Jones PES predict the existence of trapping under normal incidence conditions also, but for incidence energies up to 0.1 eV.³⁰ Considering all these recent calculations and our new AIMD results, the lack of trapping in the molecular simulations of Moron *et al.*²⁸ is possibly due to the limitations of their DFT+RPBE PES in describing both the physisorption well and the overall PES corrugation caused by the van der Waals interaction. It is worth to mention that the physisorption well (O_2 -HOPG) obtained in our DFT calculations (~ 0.11 eV for P_X , P_Y and ~ 0.09 eV for P_Z alignments) are in agreement with most recent experimental reported values (~ 0.10 eV).⁵⁷

Focusing now on the in-plane scattered molecules, Table 1 shows that the difference in the scattering probabilities between molecules with parallel (side-on) and normal (end-on) alignment is enhanced. Specifically, the probability of detecting in-plane scattered molecules coming from P_X and P_Y alignments is ~ 1.3 – 1.7 times greater than from P_Z . The fact that the total number of reflected molecules hardly depends on their initial alignment means that the alignment dependence of the in-plane probabilities is not caused by an increase in the number of trapped P_Z molecules. The reason must be related to a more efficient deviation from the scattering plane of the P_Z -aligned molecules. The outgoing azimuthal angle distributions plotted in Figure 2 for the reflected O_2 confirm that this is actually the case. Independently of the surface temperature, almost all the side-on aligned molecules are reflected with a maximal azimuthal deviation φ_s of $\pm 20^\circ$. In contrast, the azimuthal angle distributions for P_Z alignment are appreciably wider, particularly at 110 K. At 300 K, the differences seem to attenuate, but not in the in-plane range defined as $-5^\circ \leq \varphi_s \leq 5^\circ$. These results point out that end-on collisions of the molecule with the surface facilitate the transfer

of kinetic energy along the normal to the scattering plane. As a final remark, note that all the distributions are almost symmetrical as expected, indicating a reasonable statistics in our AIMD simulations. In this respect, we interpret the minimum at -7.5° for the P_z alignment at 110 K as a statistical artifact.

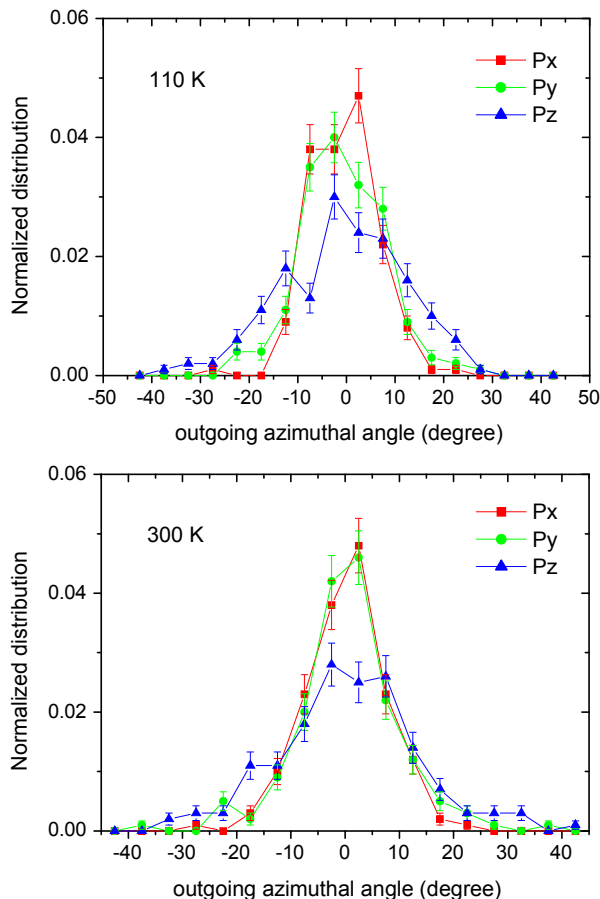


Figure 2: Outgoing azimuthal angle (φ_s) distributions of the reflected O_2 molecules at two surface temperatures (110 and 300 K). The distributions are normalized to the total number of impinging O_2 , the bin size is 5° , and the symbols are located at the central angle of the bins.

Additional information on the gas-surface interaction can be extracted from the polar angle distributions of the reflected molecules. Figure 3 shows our results at 110 and 300 K for all (left panels) and in-plane (right panels) reflected molecules. All the distributions are qualitatively similar. In each case the maximum value is located in the $25 \pm 5^\circ$ bin that contains the specular reflection angle of 22.5° . Furthermore, the distributions extend up to large outgoing angles of 70° -

80° and exhibit an asymmetrical shape around the maximum with a marked preference for angles $\theta_s > \theta_i$. This behaviour suggests that there is larger energy loss in the perpendicular than in the parallel degree of freedom. The analysis presented in section 3.2 confirms that this is the case. Both the total and in-plane angular distributions are wider at 300 K than at 110 K. A similar effect was observed in experiments performed for the same system at an incidence angle of 45° and surface temperatures varying between 150 and 500 K.¹⁸ The authors explained the broadening of the angular distribution in terms of the velocity distribution of the surface atoms. At higher surface temperatures the velocity distribution is broader and leads to a major dispersion of the scattered molecules.

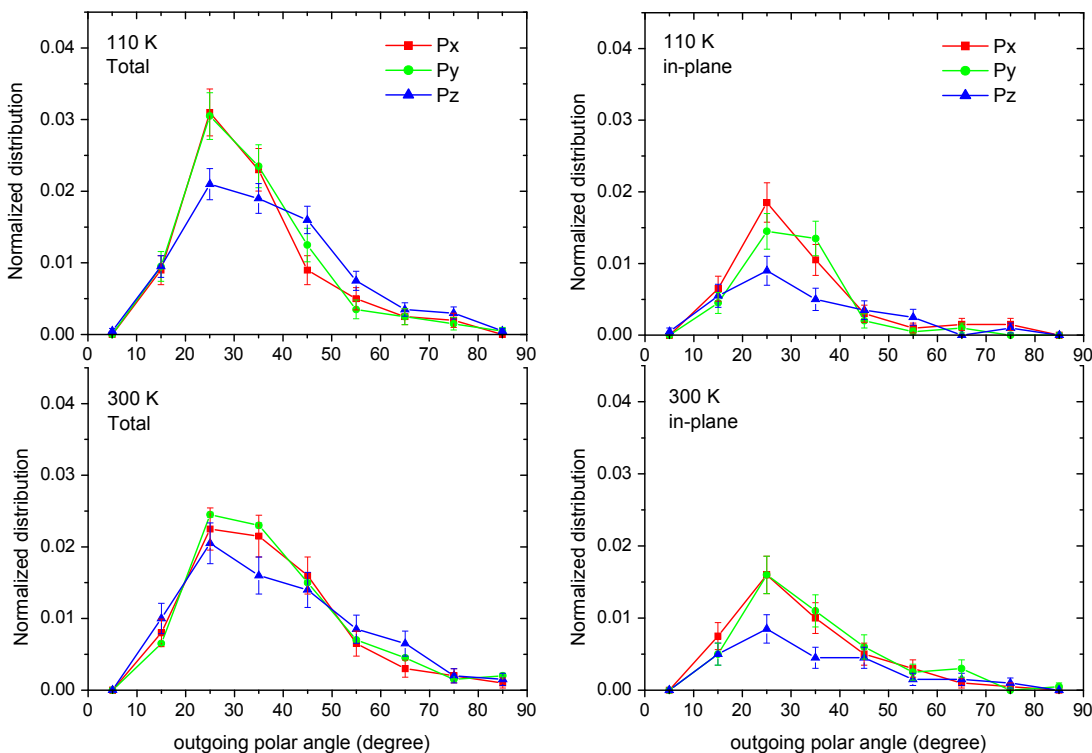


Figure 3: Outgoing polar angle (θ_s) distributions of all (left panels) and in-plane (right panels) reflected O_2 molecules at two surface temperatures (110 and 300 K). The distributions are normalized to the total number of impinging O_2 , the bin size is 10°, and the symbols are located at the central angle of the bins.

Accompanying the broadening in the angular distributions, we also observe how the alignment dependence that exists around the specular angle in the total and in-plane distributions attenuates

as the temperature increases from 110 to 300 K. For instance, the heights of the P_X , P_Y , and P_Z in-plane distributions at the $25 \pm 5^\circ$ bin decrease following this ordering at 110 K, but at 300 K the differences between the P_X and P_Y incident molecules disappear. Additionally, we observe that the in-plane P_Z distributions are wider than those of the P_X and P_Y alignments.

Different factors can contribute to the attenuation of the alignment dependence at 300 K. The aforementioned broadening of the surface atoms velocity distribution and concomitant dispersion of the colliding O_2 can effectively mask the initial alignment effects. Also an increase in the interaction time –associated to scattering after multiple collisions– can cause a partial initial-alignment memory loss. In our calculations we do observe an increase of the multi-collision scattering events from approximately 10% at 110 K to 20% at 300 K. Nonetheless, the angular distributions obtained when only single collisions are taken into account (not shown) are very similar to the ones showed in Figure 3.

Another factor we can consider is a possible reduction in the corrugation of the forces felt by the molecule in its approach to a hotter surface. The reason would be the larger and more rapid displacements of the surface atoms as the temperature increases. In order to indirectly explore this possibility, we have analyzed at what point along the AIMD trajectory the molecule deviates from the scattering plane. Figure 4 shows the time evolution of the fraction of molecules that remain in-plane ($||\varphi_s|| \leq 5^\circ$) together with the average distance of the O_2 center of mass to the topmost layer of the HOPG surface. Since most of the scattered molecules are detected during the first 1000 fs, the figure focuses on this interval from which we can extract the relevant information. During the first 300 fs, all the molecules remain in the scattering plane. At 350 fs, i.e., when the O_2 center of mass reaches heights of $\sim 3.5 \text{ \AA}$, the P_Z molecules start to deviate from it, while for the incoming P_X and P_Y molecules this deviation starts at 400 fs (i.e., heights of $\sim 3.0 \text{ \AA}$). Obviously these are the distances at which the molecule-surface interaction starts to present a non-negligible corrugation along the x, y directions. The first collision with the surface takes place at $\sim 425 \text{ fs}$ ($\sim 3.0 \text{ \AA}$) for the P_Z molecules and at $\sim 475 \text{ fs}$ ($\sim 2.5 \text{ \AA}$) for the P_X and P_Y molecules. The figure highlights that the deviation from the scattering plane occurs mainly in the part of the

trajectory close to the (classical) turning point, i.e., at surface distances at which the corrugation is the largest. The reduction in the fraction of the in-plane molecules during this first impact is stronger at 110 K than at 300 K, suggesting that the molecule-surface interaction is less corrugated at high temperatures, as hypothesized above. It is important to note that during this incoming part of the trajectory the initial alignment of the molecule remains nearly unchanged, which emphasizes the role of the initial alignment in governing the deviation from the scattering plane. In the cases of side-on approach, the small differences that are appreciable only at 110 K in the fraction of P_X and P_Y in-plane molecules are originated just after the first collision with the HOPG surface. All in all, Figure 4 remarks that the decrease in the alignment-dependence with increasing temperature is an effect that appears already during the first collision with the surface and, therefore, it must be caused mainly by the reduction of the effective corrugation at higher temperatures rather by an increase of the interaction time.

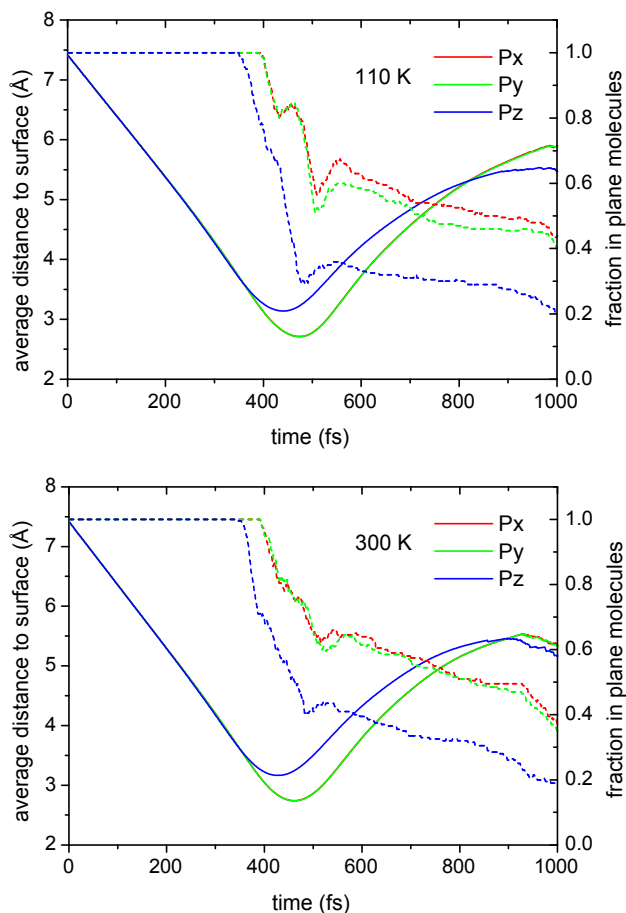


Figure 4: Time evolution of the average O_2 center of mass distance to the surface (solid lines, left Y axis) and fraction of molecules that remain within the scattering plane (dashed lines, right Y axis) during the first 1000 fs. Results presented for the different incidence alignments and surface temperatures.

3.2 Energy transfer

Figure 5 shows how the final energy of the in-plane reflected molecules is distributed between the internal and translational degrees of freedom (DOF). The results at 110 and 300 K are very similar. Regarding the dependence on the initial alignment of the molecules, the main differences appear when comparing the results of the P_Z geometry to the ones of the P_X and P_Y geometries. Whereas for the P_Z geometry the translational energy loss is $\sim 43\%$, it is a 10% lower ($\sim 33\%$), for the P_X and P_Y geometries. Remarkably, this is due to the efficient energy transfer from translational

to internal DOFs (rotational and vibrational) of the P_Z molecules upon collision with the surface and not due to the energy transfer to the surface. In fact, the P_X and P_Y molecules transfer more efficiently energy to the surface than P_Z molecules (28% of the initial energy for P_X and P_Y vs 8% of the initial energy for P_Z). However, the internal energy of the outgoing P_Z molecules is around 7 times larger than that of P_X and P_Y molecules (specifically 35% of the initial translational energy is transferred to internal DOFs for P_Z molecules and only 5% for P_X and P_Y molecules).

In addition, the lower panel of Figure 5 shows the partition of the initial and final translational energies into their perpendicular and parallel to the surface components for in-plane scattered molecules. The results show that, independent of the initial alignment, in the collision of the O_2 molecule with the thermalized HOPG surface, the component parallel to the surface of the translational energy remains practically constant. In other words, parallel momentum conservation is fulfilled, which is the assumption made by the experimentalists in order to estimate the energy transfer¹⁶ (see below). This means that only the perpendicular translational energy is efficiently lost upon collision with the surface. Interestingly, for P_Z molecules, the perpendicular translational energy loss (~ 0.10 eV) is very close to their internal energy gain (~ 0.07 eV). This indicates that for end-on molecules the energy transfer takes place between the perpendicular component of the translational energy and the internal degrees of freedom. Contrarily, for side-on molecules the loss of perpendicular energy almost equals the energy transferred to the surface.

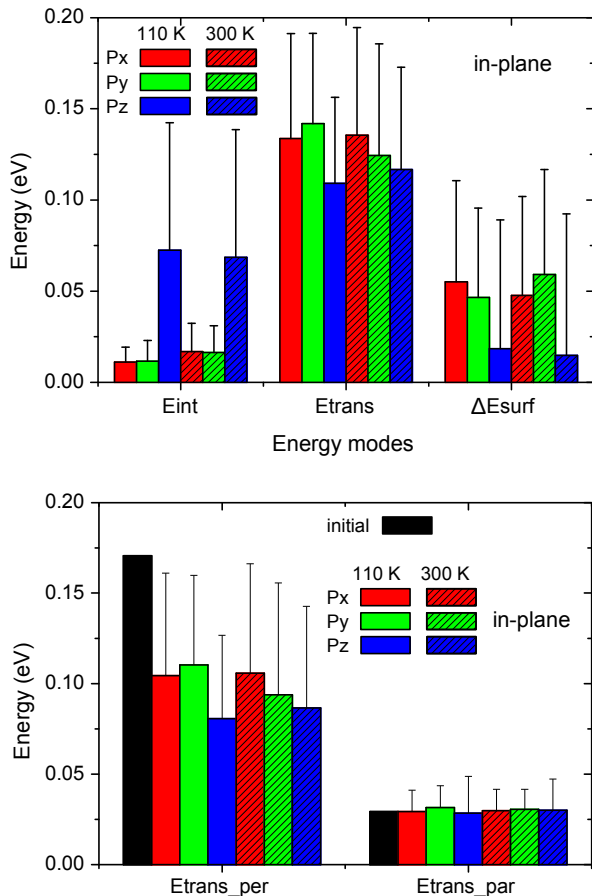


Figure 5: Top panel: Partition of the final energy of the in-plane scattered O_2 molecules into total internal energy and translational energy, and the energy transferred to the surface. Bottom panel: Partition of the final translational energy in-plane scattered O_2 molecules of into its perpendicular and parallel components. In both panels, results are shown separately for the three different initial alignments and two surface temperatures. In the bottom panel, the initial translational energy is represented by a black bars.

The energy transfer values obtained in our AIMD calculations, although not directly comparable due to the different initial conditions used, are globally in agreement with the results of recent dynamics simulations²⁹ performed on a Lenard-Jones based PES. In that work, it is observed a linear relationship between the initial energy of the molecule and the fraction of this energy transferred to the surface. They reported that 37% of the initial energy was transferred to the surface in the case of a 0.32 eV beam of O_2 molecules with an incident angle of 45° impinging on a 300 K HOPG surface. Interestingly, following the model postulated by Majumder et al,²⁹ the predicted

translational energy loss for a 0.2 eV beam of O₂ molecules with an incident angle of 45° impinging the HOPG surface would be approximately a 35% of the initial energy. This value is close to the average energy loss obtained in our calculations taking into account the three studied alignments, which is 38±5%. The small increase in the energy loss with smaller incident angle (45° vs 22.5°) is in agreement with the hard cube model predictions. Furthermore, our simulation conditions allow us to observe the differences between the ways that the energy is transferred depending of the initial alignment. These differences were not studied in the work mentioned²⁹ where initial molecule alignments were randomly obtained. Moreover, recently, a similar dependence of the rotational excitation on the alignment of O₂ molecules scattered from HOPG has been pointed out by Rutigliano and Pirani³⁰ using a PES calculated in terms of an improved Lennard-Jones (ILJ) model. Their simulations showed that molecules initially aligned perpendicular to the surface are efficiently rotational excited. However, for parallel alignments they obtained a very small change in the rotational state of the scattered molecules. Indeed, our AIMD results are consistent with the dependence of the energy transfer on the stereodynamics reported in³⁰ for the studied system.

3.3 Comparison with the experiments and discussion

To compare our results with the experiments by Kurahashi and Kondo¹⁶ it is necessary to take into account some considerations. These experiments were performed with a single spin-rotational state-selected [(J, M) = (2, 2)] O₂ beam. The rotational axis of the molecules was controlled varying the direction of the applied magnetic field. This technique allows the authors to perform measurements for helicopter and two nonequivalent cartwheel geometries. In the helicopter geometry with the rotational axis perpendicular to the surface, the molecules rotate parallel to the surface (side-on collisions). The cartwheel geometries with the rotational axis parallel to the surface contain contributions of perpendicular and parallel alignments i.e., end-on and side-on collisions. They are denoted cartwheel(x) when the rotational axis is parallel to the scattering plane and cartwheel(y) when it is perpendicular to the scattering plane. Subsequently, in order to clarify the origin of the measured alignment effects, the authors decomposed the obtained spectra into the

contributions coming from P_X , P_Y and P_Z molecular alignments. These are the initial alignments in our AIMD simulations. The decomposition was performed in terms of linear combinations of the measured spectra (helicopter $\approx P_X + P_Y$, cartwheel(x) $\approx P_Y + P_Z$ and cartwheel(y) $\approx P_X + P_Z$). It is worth to mention that the rotational energy of the molecules amount to just 0.36 meV, much lower than the translational energy, so that rotational motion is almost frozen while the molecule approaches to the surface. This allowed the experimentalists to conclude that the alignment of the molecules is much more important than their rotational motion.

Regarding the experimental incidence conditions in ref. 16, the ranges of initial translational energy and incidence polar angle (measured from surface normal) were 0.08 – 0.25 eV and $\theta_i = 0^\circ - 45^\circ$, respectively. The azimuthal direction of the molecular beam was chosen randomly. The experimental set-up only detects molecules scattered in the scattering plane (acceptance angle of 1.5°) and reflected with angles θ_s such that $\theta_i + \theta_s = 45^\circ$. Thus, the reported angular distributions as a function of θ_s were obtained varying θ_i . It is worth to mention that the maxima of the experimental angular distributions vary in a range $\theta_s \sim 24^\circ - 28^\circ$ that corresponds to $\theta_i \sim 21^\circ - 17^\circ$, depending on the molecular alignment, initial translational energy, and surface temperature. This implies small shifts from the specular direction of $\sim 3^\circ - 11^\circ$ that are ascribed to the loss of translational energy upon collision with the surface.

The large computational cost of AIMD imposes some limitations to our calculations. We are restricted to use a single angle of incidence ($\theta_i = 22.5^\circ$) and to use a bigger acceptance angle (5°) to define the in-plane scattering detection. Also, as said above, when generating the θ_s angular distributions, bins of size 10° were used. In order to reproduce the experimental conditions the azimuthal direction was varied randomly in the different simulations. For this incidence geometry, the experimental detection condition ($\theta_i + \theta_s = 45^\circ$) is fulfilled at the specular direction $\theta_s = 22.5^\circ$. In our case, this corresponds in Figure 3 to the $25 \pm 5^\circ$ detection conditions. This is also the outgoing angle for which our in-plane distributions reach the maximum value. Note that this is consistent with the experimental observations because, due to the used 10° bin size, the small angular deviations from the specular direction found in the experiments cannot be resolved in our

calculations.

The first thing to note is that, as in the experiment, in our simulations clear differences exist between the scattering probabilities and angular distributions of the P_Z geometry when compared to P_X and P_Y cases. In qualitative agreement with the experiment, the AIMD results also exhibit wider polar angle distributions for the P_Z alignment and a reduction on the alignment dependence of the scattered O_2 as the surface temperature increases from 110 to 300 K. In fact, our results are in agreement with the intensity order reported by Kurahashi and Kondo for 110 K ($P(P_X) > P(P_Y) > P(P_Z)$). At 300 K we were not able to reproduce the small differences between $P(P_X)$, $P(P_Y)$ observed in the experimental distributions but this can be attributed to the restrictive initial conditions employed in our calculations (only one incidence angle) and also to the statistical limitations of the AIMD.

In the experiments, the final energy of the molecules was not measured. However, indirect information on the final translational energy was obtained from the measured angular distributions. Assuming parallel momentum conservation, it was estimated that the loss of translational energy was $\sim 54\%$. Note that, as explained in section 3.2, the parallel momentum conservation assumption is supported by our dynamics simulations. Our results reported above (43% for P_Z and 33% for P_X and P_Y) are reasonably close to the experimental estimation. Moreover, the measured shift of 1° in the P_Z angular distributions respect to the P_X and P_Y ones was associated to differences in the energy loss experienced by the different molecular alignments. As mentioned above, our limited statistics does not allow us to resolve such small angular shifts. However, our calculations do show that the final translational energy is 10% smaller for the P_Z than for the P_X and P_Y geometries, in good agreement with the experimental difference in the final translational energies for end-on and side-on geometries deduced from the angular shifts at a somewhat lower initial energy. In this respect, it would be very interesting to perform measurements of the final rovibrational energy of the outgoing molecules to test our prediction that the reduction of the translational energy of end-on molecules is mainly governed by a more efficient excitation of the internal degrees of freedom of the molecules.

Finally, the quite good agreement obtained between the AIMD simulations and the results reported by Kurahashi and Kondo¹⁶ for aligned molecules constitutes a strong support for the interpretation of the experiments presented in that work. More precisely, it shows the correctness of the decomposition of the measured data for helicopter and cartwheel molecules into contributions coming from P_X , P_Y , and P_Z aligned molecules.

4 Conclusions

In summary, we have performed an ab initio molecular dynamics study of the alignment resolved O_2 scattering from highly oriented pyrolytic graphite. Scattering probabilities, angular distributions, and the energy transfer at two surface temperatures (110 and 300 K) of aligned molecules (P_X , P_Y and P_Z) with an incidence energy of 0.2 eV have been computed.

Our results show that trapping on this system is rather minor and that depends very weakly on surface temperature and initial alignment of the molecules. Roughly, 20% of the molecules remain trapped after the 4 ps simulation time. Additionally, most of the reflected molecules are scattered after a single collision. Regarding the in-plane scattered molecules, and in qualitative agreement with the experimental observations, we obtain a greater probability for detection of P_X and P_Y molecules than P_Z molecules. Importantly, our results demonstrate that this is not due to an increased trapping of P_Z molecules. Instead, the main cause for this alignment dependence is the more efficient out of plane scattering of P_Z molecules. It is also worth to mention that, at 110 K surface temperature, we obtain a somewhat larger probability for scattering of P_X molecules than P_Y molecules at the specular direction, which is also in qualitative agreement with the experimental observations. In general, we obtain that the alignment dependence is less pronounced at the higher 300 K temperature than at 110 K. Our analysis shows that this is due to an effective reduction of surface corrugation at higher temperatures.

We have also performed an analysis of the alignment dependence of the final energy of the scattered molecules and its distribution among the different degrees of freedom with the following

results: (i) independent of the initial alignment, parallel momentum conservation takes place and, roughly, only the perpendicular component of the translational energy is modified upon collision with the surface, (ii) the P_Z molecules transfer a small amount of energy to the surface and acquire a large amount of internal energy, (iii) the P_X and P_Y molecules transfer much more energy to the surface but do not gain much internal energy, (iv) the final outcome is that 10 % more of translational energy is lost in the case of end-on molecules as compared to side-on molecules, which is in reasonable agreement with the experimental results.

All in all, the use of AIMD allows us to obtain a quite good agreement with the alignment dependence observed in the experiments. The inclusion of independent movement of the surface atoms during the dynamics is essential to describe accurately the effect of the surface corrugation in the scattering of the molecules. The main shortcoming of AIMD simulations is their computational cost that imposes limitations to the achieved statistical accuracy. In this respect, the atomic configurations and corresponding DFT energies obtained in these simulations can be used as input data to generate multidimensional neural network potential energy surfaces. In this way, the number of calculated trajectories could be greatly increased improving the statistical accuracy. Additionally, this will also allow to reproduce more accurately the experimental conditions of Ref.¹⁶ such as the incidence and detection geometry and also perform simulations for helicopter and cartwheel molecules. It will be also possible to perform simulations for specific azimuthal incidence conditions. In this way, it could be investigated the difference of the scattering behavior when the molecule impinges along zigzag or armchair directions of the benzene ring. The results obtained in the present work constitute a strong support to overtake such program of research.

5 Acknowledgments

We acknowledge financial support by the Gobierno Vasco-UPV/EHU project IT1246-19, and the Spanish Ministerio de Ciencia, Innovación y Universidades (Grant No. FIS2016-76471-P). This research was conducted in the scope of the Transnational Common Laboratory (LTC) “Quantum-

ChemPhys – Theoretical Chemistry and Physics at the Quantum Scale”. Computational resources were provided by the DIPC computing center.

References

- (1) Okada, M. Supersonic molecular beam experiments on surface chemical reactions. *The Chemical Record* **2014**, *14*, 775–790.
- (2) Jiang, B.; Guo, H. Dynamics in reactions on metal surfaces: A theoretical perspective. *The Journal of Chemical Physics* **2019**, *150*, 180901.
- (3) Kroes, G.-J. Frontiers in Surface Scattering Simulations. *Science* **2008**, *321*, 794–797.
- (4) Kleyn, A. W. Molecular beams and chemical dynamics at surfaces. *Chem. Soc. Rev.* **2003**, *32*, 87–95.
- (5) Okada, M.; Kasai, T. Molecular orientation effects in gas-surface dynamical processes. *The European Physical Journal B* **2010**, *75*, 71–79.
- (6) Kuipers, E. W.; Tenner, M. G.; Kleyn, A. W.; Stolte, S. Observation of steric effects in gas-surface scattering. *Nature* **1988**, *334*, 420–422.
- (7) Kuipers, E. W.; Tenner, M. G.; Kleyn, A. W.; Stolte, S. Steric effects for NO/Pt(111) adsorption and scattering. *Phys. Rev. Lett.* **1989**, *62*, 2152–2155.
- (8) Lahaye, R. J. W. E.; Stolte, S.; Holloway, S.; Kleyn, A. W. Orientation and energy dependence of NO scattering from Pt(111). *The Journal of Chemical Physics* **1996**, *104*, 8301–8311.
- (9) Kneitz, S.; Gemeinhardt, J.; Steinrück, H.-P. A molecular beam study of the adsorption dynamics of CO on Ru(0001), Cu(111) and a pseudomorphic Cu monolayer on Ru(0001). *Surface Science* **1999**, *440*, 307 – 320.

- (10) Riedmüller, B.; Ciobîcă, I.; Papageorgopoulos, D.; Berenbak, B.; van Santen, R.; Kleyn, A. The dynamic interaction of CO with Ru(0001) in the presence of adsorbed CO and hydrogen. *Surface Science* **2000**, *465*, 347 – 360.
- (11) Lončarić, I.; Fuchsel, G.; Juaristi, J. I.; Saalfrank, P. Strong anisotropic interaction controls unusual sticking and scattering of CO at Ru(0001). *Phys. Rev. Lett.* **2017**, *119*, 146101.
- (12) Vattuone, L.; Savio, L.; Pirani, F.; Cappelletti, D.; Okada, M.; Rocca, M. Interaction of rotationally aligned and of oriented molecules in gas phase and at surfaces. *Prog. Surf. Sci.* **2010**, *85*, 92–160.
- (13) Kurahashi, M.; Yamauchi, Y. Steric effect in O₂ sticking on Al(111): Preference for parallel geometry. *Phys. Rev. Lett.* **2013**, *110*.
- (14) Kurahashi, M. Oxygen adsorption on surfaces studied by a spin- and alignment-controlled O₂ beam. *Prog. Surf. Sci.* **2016**, *91*, 29–55.
- (15) Godsi, O.; Corem, G.; Alkoby, Y.; Cantin, J. T.; Krems, R. V.; Somers, M. F.; Meyer, J.; Kroes, G.-J.; Maniv, T.; Alexandrowicz, G. A general method for controlling and resolving rotational orientation of molecules in molecule-surface collisions. *Nat. Commun.* **2017**, *8*, 15357.
- (16) Kurahashi, M.; Kondo, T. Alignment-resolved O₂ scattering from highly oriented pyrolytic graphite and LiF(001) surfaces. *Phys. Rev. B* **2019**, *99*, 045439.
- (17) McKee, D.; McCarroll, B. The reactivity of graphite surfaces with atoms and molecules of hydrogen, oxygen and nitrogen. *Carbon* **1972**, *10*, 328.
- (18) Oh, J.; Kondo, T.; Arakawa, K.; Saito, Y.; Hayes, W. W.; Manson, J. R.; Nakamura, J. Angular intensity distribution of a molecular oxygen beam scattered from a graphite surface. *J. Phys. Chem. A* **2011**, *115*, 7089–7095.

- (19) Hayes, W. W.; Oh, J.; Kondo, T.; Arakawa, K.; Saito, Y.; Nakamura, J.; Manson, J. R. Scattering of O₂ from a graphite surface. *J. Phys.: Condens. Matter* **2012**, *24*, 104010.
- (20) Murray, V. J.; Marshall, B. C.; Woodburn, P. J.; Minton, T. K. Inelastic and reactive scattering dynamics of hyperthermal O and O₂ on hot vitreous carbon surfaces. *J. Phys. Chem. C* **2015**, *119*, 14780–14796.
- (21) Bagsican, F. R.; Winchester, A.; Ghosh, S.; Zhang, X.; Ma, L.; Wang, M.; Murakami, H.; Talapatra, S.; Vajtai, R.; Ajayan, P. M. et al. Adsorption energy of oxygen molecules on graphene and two-dimensional tungsten disulfide. *Sci. Rep.* **2017**, *7*.
- (22) Dubský, J.; Beran, S. Quantum chemical study of oxygen adsorption on graphite. *Surf. Sci.* **1979**, *79*, 53–62.
- (23) Lamoen, D.; Persson, B. N. J. Adsorption of potassium and oxygen on graphite: A theoretical study. *J. Chem. Phys.* **1998**, *108*, 3332–3341.
- (24) Incze, A.; Pasturel, A.; Chatillon, C. Oxidation of graphite by atomic oxygen: a first-principles approach. *Surf. Sci.* **2003**, *537*, 55–63.
- (25) Giannozzi, P.; Car, R.; Scoles, G. Oxygen adsorption on graphite and nanotubes. *J. Chem. Phys.* **2003**, *118*, 1003–1006.
- (26) Paci, J. T.; Upadhyaya, H. P.; Zhang, J.; Schatz, G. C.; Minton, T. K. Theoretical and experimental studies of the reactions between hyperthermal O(³P) and graphite: Graphene-Based direct dynamics and beam-surface scattering approaches. *J. Phys. Chem. A* **2009**, *113*, 4677–4685.
- (27) Morón, V.; Gamallo, P.; Sayós, R. DFT and kinetics study of O/O₂ mixtures reacting over a graphite (0001) basal surface. *Theor. Chem. Acc.* **2011**, *128*, 683–694.
- (28) Morón, V.; Martin-Gondre, L.; Gamallo, P.; Sayós, R. Dynamics of the oxygen molecules

- scattered from the graphite (0001) surface and comparison with experimental data. *J. Phys. Chem. C* **2012**, *116*, 21482–21488.
- (29) Majumder, M.; Gibson, K. D.; Sibener, S. J.; Hase, W. L. Chemical dynamics simulations and scattering experiments for O₂ collisions with graphite. *J. Phys. Chem. C* **2018**, *122*, 16048–16059.
- (30) Rutigliano, M.; Pirani, F. On the influence of rotational motion of oxygen molecules on the scattering from graphite surfaces. *J. Phys. Chem. C* **2019**, *123*, 11752–11762.
- (31) Kresse, G.; Furthmüller, J. Efficiency of ab-initio total energy calculations for metals and semiconductors using a plane-wave basis set. *Comput. Mater. Sci.* **1996**, *6*, 15–50.
- (32) Kresse, G.; Furthmüller, J. Efficient iterative schemes for ab-initio total-energy calculations using a plane-wave basis set. *Physical Review B* **1996**, *54*, 11169–11186.
- (33) Perdew, J. P.; Burke, K.; Ernzerhof, M. Generalized gradient approximation made simple. *Physical Review Letters* **1996**, *77*, 3865–3868.
- (34) Grimme, S.; Antony, J.; Ehrlich, S.; Krieg, H. A consistent and accurate ab initio parametrization of density functional dispersion correction (DFT-D) for the 94 elements H-Pu. *J. Chem. Phys.* **2010**, *132*, 154104.
- (35) Grimme, S.; Ehrlich, S.; Goerigk, L. Effect of the damping function in dispersion corrected density functional theory. *J. Comput. Chem.* **2011**, *32*, 1456–1465.
- (36) Blöchl, P. E. Projector augmented-wave method. *Phys. Rev. B* **1994**, *50*, 17953.
- (37) Kresse, G.; Joubert, D. From ultrasoft pseudopotentials to the projector augmented-wave method. *Phys. Rev. B* **1999**, *59*, 1758–1775.
- (38) Monkhorst, H. J.; Pack, J. D. Special points for Brillouin-zone integrations. *Physical Review B* **1976**, *13*, 5188–5192.

- (39) Baskin, Y.; Meyer, L. Lattice constants of graphite at low temperatures. *Phys. Rev.* **1955**, *100*, 544–544.
- (40) Rêgo, C. R. C.; Oliveira, L. N.; Tereshchuk, P.; Silva, J. L. F. D. Comparative study of van der Waals corrections to the bulk properties of graphite. *J. Phys.: Condens. Matter* **2015**, *27*, 415502.
- (41) Lebedeva, I. V.; Lebedev, A. V.; Popov, A. M.; Knizhnik, A. A. Comparison of performance of van der Waals-corrected exchange-correlation functionals for interlayer interaction in graphene and hexagonal boron nitride. *Comput. Mater. Sci.* **2017**, *128*, 45–58.
- (42) Huber, K.; Herzberg, G. *Constants of diatomic molecules. In: Molecular Spectra and Molecular Structure.*; Springer, Boston, MA, 1979.
- (43) Groß, A.; Dianat, A. Hydrogen dissociation dynamics on precovered Pd surfaces: Langmuir is still right. *Phys. Rev. Lett.* **2007**, *98*, 206107.
- (44) Nattino, F.; Díaz, C.; Jackson, B.; Kroes, G.-J. Effect of surface motion on the rotational quadrupole alignment parameter of D_2 reacting on Cu(111). *Phys. Rev. Lett.* **2012**, *108*, 236104.
- (45) Nattino, F.; Ueta, H.; Chadwick, H.; van Reijzen, M. E.; Beck, R. D.; Jackson, B.; van Hemert, M. C.; Kroes, G.-J. Ab Initio molecular dynamics calculations versus quantum-state-resolved experiments on $CHD_3 + Pt(111)$: New insights into a prototypical gas surface reaction. *J. Phys. Chem. Lett.* **2014**, *5*, 1294–1299.
- (46) Kolb, B.; Guo, H. Communication: Energy transfer and reaction dynamics for DCI scattering on Au(111): An ab initio molecular dynamics study. *J. Chem. Phys.* **2016**, *145*, 011102.
- (47) Novko, D.; Lončarić, I.; Blanco-Rey, M.; Juaristi, J. I.; Alducin, M. Energy loss and surface temperature effects in ab initio molecular dynamics simulations: N adsorption on Ag(111) as a case study. *Phys. Rev. B* **2017**, *96*, 085437.

- (48) Zhou, X.; Kolb, B.; Luo, X.; Guo, H.; Jiang, B. Ab Initio molecular dynamics study of dissociative chemisorption and scattering of CO₂ on Ni(100): Reactivity, energy transfer, steering dynamics, and lattice effects. *J. Phys. Chem. C* **2017**, *121*, 5594–5602.
- (49) Zhou, L.; Jiang, B.; Alducin, M.; Guo, H. Communication: Fingerprints of reaction mechanisms in product distributions: Eley-Rideal-type reactions between D and CD₃/Cu(111). *J. Chem. Phys.* **2018**, *149*, 031101.
- (50) Füchsel, G.; Zhou, X.; Jiang, B.; Juaristi, J. I.; Alducin, M.; Guo, H.; Kroes, G.-J. Reactive and nonreactive scattering of HCl from Au(111): An ab initio molecular dynamics study. *J. Phys. Chem. C* **2019**, *123*, 2287–2299.
- (51) Nosé, S. A unified formulation of the constant temperature molecular dynamics methods. *J. Chem. Phys.* **1984**, *81*, 511–519.
- (52) Hoover, W. G. Canonical dynamics: Equilibrium phase-space distributions. *Phys. Rev. A* **1985**, *31*, 1695–1697.
- (53) Beeman, D. Some multistep methods for use in molecular dynamics calculations. *J. Comput. Phys.* **1976**, *20*, 130–139.
- (54) Blanco-Rey, M.; Juaristi, J. I.; Díez Muiño, R.; Busnengo, H. F.; Kroes, G. J.; Alducin, M. Electronic friction dominates hydrogen hot-atom relaxation on Pd(100). *Phys. Rev. Lett.* **2014**, *112*, 103203.
- (55) Novko, D.; Blanco-Rey, M.; Juaristi, J. I.; Alducin, M. *Ab Initio* molecular dynamics with simultaneous electron and phonon excitations: Application to the relaxation of hot atoms and molecules on metal surfaces. *Phys. Rev. B* **2015**, *92*, 201411.
- (56) Novko, D.; Blanco-Rey, M.; Alducin, M.; Juaristi, J. I. Surface electron density models for accurate *Ab Initio* molecular dynamics with electronic friction. *Phys. Rev. B* **2016**, *93*, 245435.

- (57) Ulbricht, H.; Zacharia, R.; Cindir, N.; Hertel, T. Thermal desorption of gases and solvents from graphite and carbon nanotube surfaces. *Carbon* **2006**, *44*, 2931 – 2942.

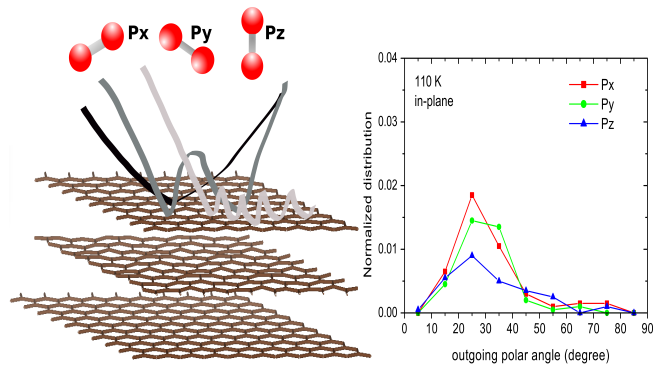


Figure 6: TOC Graphic